

THERMAL ANALYSIS OF PARTICLE RATIOS AND p_{\perp} SPECTRA AT RHIC*

WOJCIECH FLORKOWSKI, WOJCIECH BRONIOWSKI
AND MARIUSZ MICHALEC

H. Niewodniczański Institute of Nuclear Physics,
Radzikowskiego 152, 31-342 Kraków, Poland

(Received December 5, 2001)

The thermal model of particle production is used to analyze the particle ratios and the p_{\perp} spectra measured recently at RHIC. Our fit of the particle ratios yields the temperature at the chemical freeze-out $T_{\text{chem}} = 165 \pm 7$ MeV with the corresponding baryon chemical potential $\mu_{\text{chem}}^B = 41 \pm 5$ MeV. The quality of the fit shows that the model works well for RHIC. The p_{\perp} spectra are evaluated in an approach which takes into account the modifications of the initial thermal distributions by the secondary decays of resonances. All two- and three-body decays are included. This leads to an effective “cooling” of the spectra in the data region by about 30–40 MeV. We find that the pion spectrum is characterized by the inverse slope which agrees well with the value inferred from the RHIC data.

PACS numbers: 25.75.Dw, 21.65.+f, 14.40.-n

1. Introduction

Recently, a successful description of the particle ratios measured in relativistic heavy-ion collisions has been achieved in the framework of so-called thermal models [1–9]. An important ingredient of this approach is the proper inclusion of the hadronic resonances, whose decays contribute in an essential way to the final multiplicities of the observed hadrons. In the first part of this paper the simple thermal model is used to find the optimal values of the thermodynamic parameters characterizing the ratios measured at RHIC. In the second part we calculate the p_{\perp} spectra of hadrons in the thermal model, including all resonances and using an analytic formula. The spectra, besides the original thermal distribution, receive large contributions from the decaying resonances. The inclusion of all possible decays is important, since

* Research supported in part by the Polish State Committee for Scientific Research, grant no. 2 P03B 09419

only in that way one can obtain a clean separation and identification of other effects such as expansion, flow [10–16], or medium modifications [17–19], which influence the final shape of the p_{\perp} distributions. The present analysis computes the spectra in a static fireball, and is introductory to the work of Ref. [20], where the effects of expansion are incorporated and very good agreement with experiment is achieved.

2. Ratios of hadron multiplicities

In the thermal model the particle densities are calculated from the ideal-gas expression

$$n_i = \frac{g_i}{2\pi^2} \int_0^{\infty} \frac{p^2 dp}{\exp \left[(E_i - \mu_{\text{chem}}^{\text{B}} B_i - \mu_{\text{chem}}^{\text{S}} S_i - \mu_{\text{chem}}^{\text{I}} I_i) / T_{\text{chem}} \pm 1 \right]}, \quad (1)$$

where g_i is the spin degeneracy factor of the i^{th} hadron, B_i , S_i , I_i are the baryon number, strangeness, and the third component of isospin, and $E_i = \sqrt{p^2 + m_i^2}$. The quantities $\mu_{\text{chem}}^{\text{B}}$, $\mu_{\text{chem}}^{\text{S}}$ and $\mu_{\text{chem}}^{\text{I}}$ are the chemical potentials enforcing the appropriate conservation laws. We note that Eq. (1) is used to calculate the “primordial” densities of stable hadrons and resonances at the chemical freeze-out. The final multiplicities receive contributions from the primordial stable hadrons, as well as from the secondary hadrons produced by sequential decays of resonances after the freeze-out. We include *all* light-flavor hadrons (with the appropriate branching ratios) listed in the newest review of particle physics [21]. We neglect the finite-size and excluded volume corrections¹. The temperature, T_{chem} , and the baryonic chemical potential, $\mu_{\text{chem}}^{\text{B}}$, are fitted by minimizing the expression

$$\chi^2 = \sum_{k=1}^n \frac{(R_k^{\text{exp}} - R_k^{\text{therm}})^2}{\sigma_k^2},$$

where R_k^{exp} is the k^{th} measured ratio, σ_k is the corresponding error, and R_k^{therm} is the same ratio as determined from the thermal model. The potentials $\mu_{\text{chem}}^{\text{S}}$ and $\mu_{\text{chem}}^{\text{I}}$ are determined by the two requirements: the initial strangeness of the system is zero, and the ratio of the baryon number to the electric charge is the same as in the colliding nuclei.

¹ If the sizes of mesons and baryons are equal, the excluded volume corrections practically cancel in the particle ratios. This is due to the fact that the overwhelming majority of hadrons is heavy and may be treated as classical particles. In this case we may replace the Fermi–Dirac (Bose–Einstein) distribution function in (1) by the Boltzmann distribution function, for which the excluded volume corrections factorize. We have checked that the use of the classical statistics changes the values of the thermodynamic parameters by less than 3%.

TABLE I

Our fit to the particle ratios measured at RHIC.

	Thermal model	Experiment
T_{chem} [MeV]	165 ± 7	
$\mu_{\text{chem}}^{\text{B}}$ [MeV]	41 ± 5	
$\mu_{\text{chem}}^{\text{S}}$ [MeV]	9	
$\mu_{\text{chem}}^{\text{I}}$ [MeV]	-1	
χ^2/n	0.97	
π^-/π^+	1.02	1.00 ± 0.02 [24], 0.99 ± 0.02 [25]
\bar{p}/π^-	0.09	0.08 ± 0.01 [26]
K^-/K^+	0.92	0.88 ± 0.05 [27], 0.78 ± 0.12 [28] 0.91 ± 0.09 [24], 0.92 ± 0.06 [25]
K^-/π^-	0.16	0.15 ± 0.02 [27]
K_0^*/h^-	0.046	0.060 ± 0.012 [27, 29]
\bar{K}_0^*/h^-	0.041	0.058 ± 0.012 [27, 29]
\bar{p}/p	0.65	0.61 ± 0.07 [26], 0.54 ± 0.08 [28] 0.60 ± 0.07 [24], 0.61 ± 0.06 [25]
$\bar{\Lambda}/\Lambda$	0.69	0.73 ± 0.03 [27]
$\bar{\Xi}/\Xi$	0.76	0.82 ± 0.08 [27]

Table I presents our fit to the particle ratios measured at RHIC. In our calculation, the identical ratios measured by different groups are treated separately in the definition of χ^2 (number of points $n = 16$). In this way the measurements done by different groups enter independently. Very similar results are obtained if we first average the results of different groups to obtain the most likely value for each considered ratio. Our optimal value of $T_{\text{chem}} = 165 \pm 7$ MeV is consistent with the value of the critical temperature as inferred from the lattice simulations of QCD (with three massless flavors $T_{\text{C}} = 154 \pm 8$ MeV, whereas with two massless flavors $T_{\text{C}} = 173 \pm 8$ MeV [22]). We have also calculated other characteristics of the freeze-out. In particular, we find the energy density $\varepsilon = 0.5$ GeV/fm³, the pressure $P = 0.08$ GeV/fm³, and the baryon density $\rho_{\text{B}} = 0.02$ fm⁻³. Our calculation confirms the Cleymans–Redlich conjecture [5] that the energy per hadron at the chemical

freeze-out is 1 GeV (our approach yields $\langle E \rangle / \langle N \rangle = 1.0$ GeV). We observe, however, that the average energy per baryon is much larger than the average energy per meson: $\langle E_B \rangle / \langle N_B \rangle = 1.6$ GeV and $\langle E_M \rangle / \langle N_M \rangle = 0.9$ GeV. Similar differences occur also for other heavy-ion collisions studied at AGS and SPS. They are caused by the different growth rates of the meson and baryon mass spectra [23]. In addition, we find that the ratios $\bar{\Lambda}/\Lambda$ and $\bar{\Xi}/\Xi$ are practically unaffected by the weak decays. In conclusion, the thermal model works well for the RHIC particle ratios, with thermal parameters assuming anticipated values.

We note that our T_{chem} is 9 MeV lower than 174 MeV of Ref. [30], and 25 MeV lower than 190 MeV obtained in Ref. [31]. Nevertheless, the results of the three calculations are consistent within errors, as displayed in Fig. 1. An interesting feature shown in Fig. 1 is the characteristic valley of the optimal parameters. The shape of this valley indicates that the quality of the fit does not change if we moderately increase or decrease both T_{chem} and μ_{chem}^B .

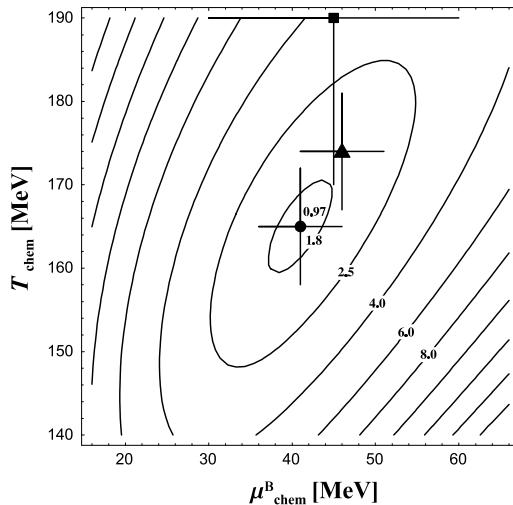


Fig. 1. The contour plot of our χ^2/n treated as a function of T_{chem} and μ_{chem}^B . Our result (black circle), the result of Ref. [30] (black triangle), and the fit of Ref. [31] (black square) are all shown with the corresponding errors.

3. Transverse-momentum spectra

Next, we come to the discussion of the p_T spectra. Similarly to the particle multiplicities, the momentum spectra of the observed hadrons contain two contributions. The first, “primordial” contribution is purely thermal and is described by distribution functions characterized by the thermodynamic

parameters at freeze-out. The second contribution comes from sequential decays of the resonances. Since a substantial part of the produced particles comes from the decays, one may expect that the measured spectra are significantly changed by this effect. Indeed, it has been already known for a long time that the resonance decays modify the low- p_T spectrum, due to the limited phase space of the emitted particles [32–34]. So far, however, a rather limited number of the resonances has been included in such analysis. We take into account all two- and three-body hadronic decays. In this study we neglect other effects which can change the spectra, such as expansion or flow.

Below we sketch our method of dealing with two- and three-body decays. The initial momentum distribution function of a resonance in the fireball rest frame, $f(k)$, as well as the momentum distribution of the emitted particle in the resonance's rest frame, are isotropic. The latter is true, since we average over all possible polarization states. Thus, in the case of a two-body decay, the spectrum of the emitted particle (denoted by index 1) is obtained from the expression

$$\tilde{f}_1(|\mathbf{q}|) = b \frac{2J_R + 1}{2J_1 + 1} \int d^3k f(k) \int \frac{d^3\mathbf{p}}{4\pi p^{*2}} \delta(|\mathbf{p}| - p^*) \delta^{(3)}(\hat{L}_k \mathbf{p} - \mathbf{q}), \quad (2)$$

where \mathbf{p} is the momentum of the emitted particle in the rest frame of the resonance, and \hat{L}_k is the Lorentz transformation to the fireball rest frame,

$$\hat{L}_k \mathbf{p} = \mathbf{p} + \left[(\gamma_k - 1) v_k^2 \mathbf{v}_k \cdot \mathbf{p} + \gamma_k E^* \right] \mathbf{v}_k. \quad (3)$$

Here \mathbf{k} is the momentum of the resonance in the fireball, $\mathbf{v}_k = \mathbf{k} / \sqrt{k^2 + m_R^2}$, and $\gamma_k = (1 - v_k^2)^{-1/2}$. In Eq. (2) p^* is the magnitude of \mathbf{p} and $E^* = \sqrt{p_*^2 + m_1^2}$. The standard formula gives

$$p^* = \frac{\left[(m_R^2 - (m_1 - m_2)^2) (m_R^2 - (m_1 + m_2)^2) \right]^{1/2}}{2m_R}, \quad (4)$$

where m_R is the mass of the resonance, whereas m_1 and m_2 are the masses of the emitted particles. The quantity b is the branching ratio for the considered channel, and J_R and J_1 are the spins of the resonance and particle 1, respectively. The physical interpretation of Eq. (2) is clear: the isotropic distribution of particle 1 in the resonance rest frame, $\delta(|\mathbf{p}| - p^*) / (4\pi p^{*2})$, is boosted to the fireball frame, and there folded with the resonance distribution $f(k)$.

In order to write Eq. (2) in a more compact form, we do the change of variables:

$$\mathbf{p}' = \hat{L}_k \mathbf{p}, \quad d^3 p = \frac{E_p}{E_{p'}} d^3 p' = \frac{E^*}{E_q} d^3 p'. \quad (5)$$

The integration over p' in (2) becomes trivial and we find

$$\tilde{f}_1(|\mathbf{q}|) = b \frac{2J_R + 1}{2J_1 + 1} \frac{1}{4\pi p^{*2}} \frac{E^*}{E_q} \int d^3 k f(k) \delta\left(\left|\hat{L}_k^{-1} \mathbf{q}\right| - p^*\right). \quad (6)$$

Since the quantity $\hat{L}_k^{-1} \mathbf{q}$ is the momentum of the emitted particle in the reference frame connected with the resonance, we may rewrite Eq. (6) in the explicitly Lorentz-covariant way

$$\tilde{f}_1(|\mathbf{q}|) = b \frac{2J_R + 1}{2J_1 + 1} \frac{1}{4\pi p^*} \frac{1}{E_q} \int d^3 k f(k) \delta\left(\frac{k^\mu q_\mu}{m_R} - E^*\right). \quad (7)$$

Here k^μ and q^μ are the four-momenta of the resonance and of the emitted particle, respectively. We note that Eq. (7) was used previously by Sollfrank, Koch, and Heinz [32]. In their approach, however, no assumptions about the isotropic emission were made, so $f(k)$ and consequently $\tilde{f}_1(q)$ were treated as the functions of two arguments: rapidity and transverse momentum. In our approach $f(k)$ and $\tilde{f}_1(q)$ depend only on the magnitude of the three-momenta, and integration over the polar and azimuthal angles in (7) can be done analytically. This leads to a simple expression

$$\tilde{f}_1(q) = b \frac{2J_R + 1}{2J_1 + 1} \frac{m_R}{2E_q p^* q} \int_{k_-(q)}^{k_+(q)} dk k f(k), \quad (8)$$

where the limits of the integration are $k_\pm(q) = m_R |E^* q \pm p^* E_q| / m_1^2$. Eq. (8) is a relativistic generalization of the formula derived in Ref. [34]. Its simplicity turns out to be especially important in the numerical treatment of the sequential decays.

In the case of three-body decays we can follow the same steps as above, with the extra modification connected with the fact that different values of p^* are possible now. This introduces an additional integration in Eq. (2). The distribution of the allowed values of p^* may be obtained from the phase-space integral

$$N \int \frac{d^3 p_1}{E_{p_1}} \frac{d^3 p_2}{E_{p_2}} \frac{d^3 p_3}{E_{p_3}} \delta\left(m_R - E_{p_1} - E_{p_2} - E_{p_3}\right) \delta^{(3)}(\mathbf{p}_1 + \mathbf{p}_2 + \mathbf{p}_3) |M|^2, \quad (9)$$

where $\mathbf{p}_1, \mathbf{p}_2$ and \mathbf{p}_3 are the momenta of the emitted particles, E_{p_1}, E_{p_2} and E_{p_3} are the corresponding energies (all measured in the resonance rest frame), M is the matrix element describing the three-body decay, and N is the normalization constant. For sake of simplicity we assume, similarly as in [32], that M can be approximated by a constant. Operationally, the final expression for three-body decays is a folding of two-body decays over p^* with a weight following from elementary considerations based on Eq. (9).

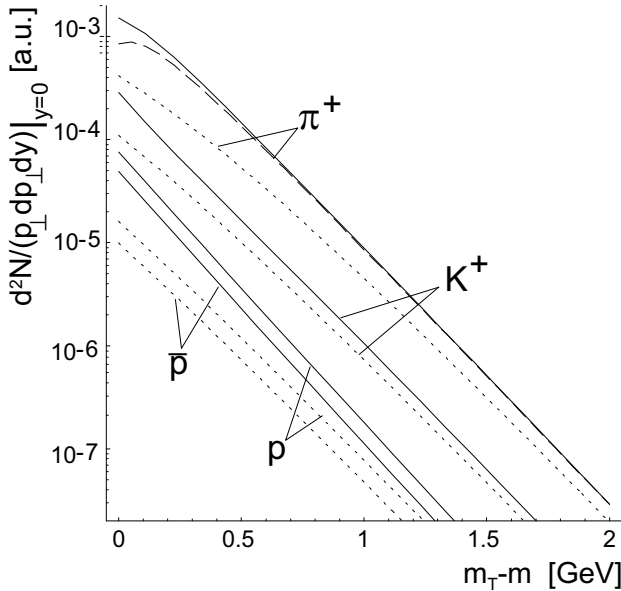


Fig. 2. The transverse-mass distributions of pions, kaons, protons and anti-protons.

Our numerical procedure is as follows: We initialize the spectra of all hadrons as given by the thermal model. Next, we start from the heaviest particle, and proceed with the decay, thus feeding the spectra of the products. We repeat this step for all particles, going down with the mass, until all resonances are taken into account. Our results for the p_{\perp} spectra are shown in Fig. 2. The initial thermal distributions are represented by the dashed lines, whereas the final distributions are represented by the solid lines. In the case of pions the long-dashed line shows the result of including two-body decays only. We observe that the final distributions of hadrons are considerably steeper than the original distributions. We term this phenomenon as “cooling” of the spectra by secondary decays. For the pions the initial inverse slope, calculated in the range $0.3 \text{ GeV} < p_{\perp} < 0.9 \text{ GeV}$ [35], equals 219 MeV. Hadronic decays cool it by 34 MeV down to 185 MeV.

The last value agrees well with the measurement of the PHENIX Collaboration [35]². The inverse slopes obtained for other hadrons are smaller than those inferred from the data. Definitely, other processes influence the observed spectra.

Our calculation does not show any peaked low- p_{\perp} enhancement in the pion spectrum. It would, if for instance we had included only the $\Delta(1232)$ decays. However, with all decays included, the increase of the spectrum is uniform due to the fact that different decays populate different momenta. The shape of the pion spectrum in Fig. 2 is concave, thus the thermal model does not reproduce the experimental convex shape [35]. One can see that the contributions from the three-body decays to the pion spectrum are important at small momenta, however, they are smaller than the contributions from the two-body decays. The impact of three-body decays on other spectra is negligible.

Certainly, the expansion or flow effects further modify the spectra. Their inclusion is necessary to obtain the complete agreement with the data [20]. However, the effect of “cooling” from secondary decays described in this paper is an important ingredient of any analysis of momentum spectra in relativistic heavy-ion collisions.

REFERENCES

- [1] P. Braun-Munzinger, J. Stachel, J.P. Wessels, N. Xu, *Phys. Lett.* **B344**, 43 (1995); *Phys. Lett.* **B365**, 1 (1996).
- [2] J. Cleymans, D. Elliott, H. Satz, R.L. Thews, *Z. Phys.* **74**, 319 (1997).
- [3] P. Braun-Munzinger, I. Heppe, J. Stachel, *Phys. Lett.* **B465**, 15 (1999).
- [4] J. Rafelski, J. Letessier, A. Tounsi, *Acta Phys. Pol.* **B28**, 2841 (1997).
- [5] J. Cleymans, K. Redlich, *Phys. Rev. Lett.* **81**, 5284 (1998).
- [6] G.D. Yen, M.I. Gorenstein, *Phys. Rev.* **C59**, 2788 (1999).
- [7] F. Becattini, J. Cleymans, A. Keranen, E. Suhonen, K. Redlich, *Phys. Rev.* **C64**, 024901 (2001).
- [8] F. Becattini, J. Cleymans, A. Keranen, E. Suhonen, K. Redlich, [hep-ph/0011322](https://arxiv.org/abs/hep-ph/0011322).

² Contrary to a naive expectation, the inverse slopes of the thermal distributions in Fig. 2 (dotted lines) do not correspond to the physical temperature characterizing the thermal distribution f . This effect is induced by the presence of m_{\perp} as a pre-factor multiplying the thermal distribution in the expression for the yield: $dN/(m_T dm_T dy) \sim m_{\perp} \cosh(y) f(m_{\perp} \cosh(y))$. Since the values of m_{\perp} are not asymptotic, the inverse slopes obtained in the region of $p_{\perp} \sim 0.5-1$ GeV are considerably higher than the temperature.

- [9] M. Gaździcki, *Nucl. Phys.* **A681**, 153 (2001).
- [10] E. Schnedermann, J. Sollfrank, U. Heinz, *Phys. Rev.* **C48**, 2462 (1993).
- [11] T. Csörgő, B. Lörstad, *Phys. Rev.* **C54**, 1390 (1996).
- [12] D.H. Rischke, M. Gyulassy, *Nucl. Phys.* **A697**, 701 (1996); *Nucl. Phys.* **A608**, 479 (1996).
- [13] R. Scheibl, U. Heinz, *Phys. Rev.* **C59**, 1585 (1999).
- [14] D. Teaney, J. Lauret, E.V. Shuryak, *Phys. Rev. Lett.* **86**, 4783 (2001).
- [15] P. Huovinen, P.F. Kolb, U. Heinz, P.V. Ruuskanen, S.A. Voloshin, *Phys. Lett.* **B503**, 58 (2001).
- [16] P. Huovinen, `nucl-th/0108033`.
- [17] W. Florkowski, W. Broniowski, *Phys. Lett.* **B477**, 73 (2000).
- [18] W. Florkowski, W. Broniowski, Proceedings of the International Workshop XXVIII on Gross Properties of Nuclei and Nuclear Excitations, Hirschegg, Austria, 2000, p. 275.
- [19] M. Michalec, W. Florkowski, W. Broniowski, *Phys. Lett.* **520**, 213 (2001).
- [20] W. Broniowski, W. Florkowski, *Phys. Rev. Lett.* **87**, 272302 (2001).
- [21] Particle Data Group, *Eur. Phys. J.* **C15**, 1 (2000).
- [22] F. Karsch, Proceedings of QM2001, *Nucl. Phys. A*, in print, `hep-ph/0103314`.
- [23] W. Broniowski, W. Florkowski, *Phys. Lett.* **B490**, 223 (2000).
- [24] B.B. Back, PHOBOS Collaboration, *Phys. Rev. Lett.* **87**, 102301 (2001).
- [25] I.G. Bearden, BRAHMS Collaboration, Proceedings of QM2001, *Nucl. Phys. A*, in print.
- [26] J. Harris, STAR Collaboration, Proceedings of QM2001, *Nucl. Phys. A*, in print.
- [27] H. Caines, STAR Collaboration, Proceedings of QM2001, *Nucl. Phys. A*, in print.
- [28] H. Ohnishi, PHENIX Collaboration, Proceedings of QM2001, *Nucl. Phys. A*, in print.
- [29] Z. Xu, Proceedings of QM2001, *Nucl. Phys. A*, in print, `nucl-ex/0104001`.
- [30] P. Braun-Munzinger, D. Magestro, K. Redlich, J. Stachel, *Phys. Lett.* **B518**, 41 (2001).
- [31] N. Xu, M. Kaneta, Proceedings of QM2001, *Nucl. Phys. A*, in print, `nucl-ex/0104021`.
- [32] J. Sollfrank, P. Koch, U. Heinz, *Phys. Lett.* **252**, 256 (1990).
- [33] G.E. Brown, J. Stachel, G.M. Welke, *Phys. Lett.* **B253**, 19 (1991).
- [34] W. Weinhold, Zur Thermodynamik des πN -Systems, PhD Thesis, GSI, 1995.
- [35] J. Velkovska, PHENIX Collaboration, Proceedings of QM2001, *Nucl. Phys. A*, in print, `nucl-ex/0105012`.